Improving corrosion stability and antibacterial activity of the titania coatings by plasma electrolytic oxidation

M. M. DICU[a], M. URSU[b], C. UNGUREANU[c], P. C. DICU[a], S. POPESCU[c*]
[a]*University of Pitesti, Faculty of Mechanics and Technology, Targu din Vale, No 1, 110040, Pitesti, Romania*
[b]*Renault Technologie Roumanie, Uzinei, No 1-3, 115400, Mioveni, Arges, Romania*
[c]*University Politehnica of Bucharest, Faculty of Applied Chemistry and Materials Science, Polizu no 1-7, 011061, Bucharest, Romania*

The titania (TiO_2) coatings containing Ca and P was successfully deposited on titanium substrate by plasma electrolytic oxidation (PEO) technique. The electrolyte was a mixture consisting of β-glycerophosphate disodium salt pentahydrate and calcium acetate monohydrate. The obtained surfaces were characterized using SEM, XRD, AFM, FTIR and contact angle measurements in order to obtain morphological, topographical, compositional features and wettability of the surface. The electrochemical behavior of the Ti/TiO_2 coating was tested in buffer solution. The corrosion parameters obtained from linear polarisation measurements, electrical parameters from electrochemical impedance spectroscopy and cyclic potentiodynamic polarisation were obtained. The antibacterial activity of the TiO_2 coatings against *Escherichia coli* was examined by bacterial counting method. Percentage inhibition of bacteria growth was determined by streak method. The results showed a good electrochemical stability, combined with positive results regarding their antibacterial activity and *in vitro* cytotoxicity.

(Received September 29, 2015; accepted October 28, 2015)

Keywords: Titania, Plasma electrolytic oxidation, Surface analysis, Corrosion stability, Antibacterial activity, *In vitro* cytotoxicity

1. Introduction

Titanium and its alloys are still the most used valve metal in medical applications. Although it possesses the appropriate mechanical, physical and chemical characteristics to accomplish the functions of an implant, titanium is gradually affected by body fluids, thus corrosion resistance become critical for the overall success of the treatment procedure [1, 2]. The corrosion products formed as a result of metal-biological fluids interactions have a significant connection with the biocompatibility and implant long term stability [3]. Moreover, titanium and its thin naturally formed oxide films are known to be bio-inert [4, 5].

In order to diminish these two important drawbacks, surface engineering developed solutions that involved the use of different treatments: chemical (etching, sol-gel deposition), electrochemical (anodic oxidation, micro-arc oxidation), physical (physical vapor deposition, thermal spray, plasma spraying), mechanical (machining, grinding, polishing), thermal (thermal oxidation, sintering) [6, 7]. Regarding the applied treatments for Ti surface, improving the corrosion response of Ti with TiO_2 layers are well-known to provide a better protection [8-10]. The most accepted technique for the surface modification of Ti with TiO_2 is oxidation that can be produced through various methods: in furnace at high temperature [11, 12], electrochemically anodization [13, 14], plasma-enhanced atomic layer deposition [15, 16], plasma electrolytic oxidation (PEO) [17-19].

Among all electrochemical techniques applied for changing the surface properties of metals, PEO is considered one of the most useful methods for surface modification of titanium or titanium alloys implants surface [20]. PEO is a non-expensive, simple, controllable and efficient method for formation of oxide layers with a coarse and porous structure and high cohesivity on the surface of titanium and its alloys, providing a better corrosion resistance for bulk metallic substrate and an enhanced implant fixation to the bone [21]. The PEO process has several advantages, such as a possibility to control thickness and morphology of the surface layer, ability to form coatings on complex shapes, and higher growth rates compared to conventional anodizing [17-19]. The coatings are obtained by applying high voltages to generate a sequence of short-lived microdischarges on the metal surface. When the applied voltage to a Ti substrate immersed in an electrolyte is increased to a certain point a micro-arc occurs and a TiO_2 layer on the surface is formed [22].

On the other hand, in order to minimize the bio-inertness and to improve the bioactivity of titanium implants, different solutions for enhancing their osseointegration with the bone tissue were proposed. Considering that the capability of an implant to create a strong bond with a living tissue is highly dependent on the surface physical and chemical characteristics, one of the most appropriate method is bonding bioactive substances on the surface [23-25]. In this way, bioactive materials can be incorporated into the surface layer during the PEO process by tailoring the composition of the electrolyte

solution [26, 27]. Among them, bioglasses or calcium phosphate bioactive phases such as hydroxyapatite (HAp, $Ca_{10}(PO_4)_6(OH)_2$) are often used, providing bioactivity and osteoconductivity at the interface titanium-tissue [28-32].

HAp coated titanium implants have attracted much more attention during recent decades, due to the crystallographic structure and chemical composition of Hap, similar with hard tissues. It has been proven that HAp has the advantage to induce bone regeneration and also provides better bone cells reproduction [33].

Although different methods like plasma spray, sol–gel, electrophoretic deposition, cathode deposition, laser forming and hydrothermal process were used to fabricate HAp layers with various structures [34], PEO is an advanced technique of HAp layer production that has multiple advantages. Therefore, PEO-based surface engineering methods are attractive for the formation of HA coatings on titanium substrates, including hybrid TiO_2:n-HA coatings [28].

In addition, PEO can introduce Ca and P ions into Ti surface by controlling the processing parameters such as the composition of the electrolyte, applied voltage, current density, and treatment times. A correlation between current density and electrolyte concentration used during the PEO process on titanium and proportions of anatase and rutile phases, surface morphologies, coating thicknesses was observed [35].

This study is intended to be a comprehensive approach treating all aspects regarding future use of titania coatings containing Ca and P in medical applications. These are related to morphology, topography, chemical structure, wettability, adhesion, electrochemical behavior in simulated bioliquids correlated with microbial activity and aspects related to cytotoxicity.

2. Experimental

2.1 Preparation of substrate

Titanium rectangular samples (with dimensions of 12 mm × 12 mm × 3 mm) cut from a sheet of commercially pure titanium (grade 2) were used as substrate. The chemical composition of the raw material is: Fe 0.105 %; C 0.011 %; O 0.175 %; N 0.006 %; H 0.0005 % and 99.7% Ti. The sample plates were polished gradually using #200 – #4000 SiC sandpaper, degreased and successively cleaned in an ultrasonic bath with ethanol and distilled water.

2.2 Synthesis of TiO_2 films using PEO technique

The PEO equipment was design and manufactured at the University of Pitesti. The experimental set-up consists of an insulated stainless steel electrolyte cell and a pulsed bipolar DC power supply. The titanium plate was used as anode, while a stainless steel cell was used as cathode. The electrolyte in the electrolyte cell was an aqueous solution containing 0.04 mol/l β-glycerophosphate disodium salt pentahydrate ($C_3H_7Na_2O_6P{\cdot}5H_2O$) and 0.4 mol/l calcium acetate monohydrate ($(CH_3COO)_2Ca{\cdot}H_2O$) in distilled water.

A 15 kW PEO coating deposition equipment of unit designed was used for the coating deposition. The oxidation parameters were: voltage (250V, 350V, 450V) and the oxidation time (3 min). The PEO treatments were obtained using a pulsed current regime. After the treatment, the samples were washed with distilled water and dried at room temperature.

2.3 Methods for TiO_2 ceramic coatings characterization

2.3.1. Surface characterization

Scanning electron microscopy (SEM) - The morphology of treated surfaces was observed on a Scanning Electron Microscope (SEM, Low-vacuum INSPECT S – FEI Company). The SEM equipment was operated at 15 kV.

Energy-dispersive X-ray spectroscopy (EDX) - The elemental composition was studied with energy dispersive X-ray spectrometer (EDX, Genesis-XM2) incorporated into the scanning electron microscope. EDX was performed at an acceleration voltage of 20 kV.

X-ray diffraction (XRD) – The crystalline nature of the TiO_2 coatings was analysed using a Rigaku Ultima IV wih CuKα radiation, with Parallel Beam optics, in grazing incidence geometry (angle of incidence was kept constant at 1°). The measurements were conducted in the 2θ range 20^0-80^0, step width 0.05^0 and 2s as counting time.

Atomic force microscopy (AFM) - Topographical and morphological analyses were performed with an AFM equipment A.P.E Research A100-SGS, using an ultra-sharp cantilever tip.

The Fourier transform infrared spectroscopy (FTIR) - Infrared spectra were obtained using a Spectrum 100 FT-IR spectrophotometer (Perkin Elmer) in the attenuated total transmittance mode (ATR). Spectra covering the range from 4000 to 600 cm^{-1} and 4 scans at a resolution of 4 cm^{-1} were used.

The contact angle - The surface hydrophilicity of TiO_2 films was determined with a KSV Instruments CAM 100, by measuring the static contact angle of a drop of distilled water deposited on the sample surface. The volume of the liquid was kept constant (10 μL). Each contact angle value is the average of the minimum 3 measurements. The investigation was carried out with an accuracy of ±1° at a temperature of 25 °C.

Adherence test - The experiments regarding the adherence of TiO_2 films were per-formed with a PosiTest Adhesion Tester (DeFelsko Corporation).

2.3.2 Electrochemical characterization

All electrochemical measurements were performed using one compartment cell with three electrodes: a working electrode, a platinum counter-electrode and an Ag/AgCl, KCl reference electrode connected to Autolab PGSTAT 302N potentiostat with NOVA general-purpose

electrochemical system software. The titanium with an exposed surface area of 1 cm^2 was used as the working electrode.

The electrochemical stability was determined in a buffer solution, at room temperature. The chemical composition of the solution was: NaCl 8.74 g/L; $NaHCO_3$ 0.35 g/L; $Na_2HPO_4 \cdot 12H_2O$ 0.06 g/L; NaH_2PO_4 0.06 g/L.

The following electrochemical techniques were employed:

Polarization curves were registered at ±150 mV vs. OCP, at a scan rate of 2 mV/s and corrosion parameters were computed based on Tafel plots: i_{cor} (corrosion current density), R_p (polarization resistance), E_{cor} (corrosion potential) and v_{cor} (corrosion rate).

Electrochemical impedance spectroscopy (EIS) studies were carried out at an open circuit potential. The EIS spectra were acquired in the frequency range of 0.1 − 10^5 Hz in order to obtain Nyquist plots by applying a small excitation amplitude of 10 mV.

The cyclic potentiodynamic polarisation - Cyclic curves were recorded. The electrode potential was cycled between –0.6 and + 4V, at a scan rate of 20 mV/s.

2.3.3 Antibacterial activity of TiO_2 ceramic coatings

Escherichia coli (K 12-MG1655) were cultured in a tube containing Luria Bertani (LB) medium at 37 ^oC (L.B. medium composition: peptone, 10 g/L; yeast extract 5 g/L, NaCl 5 g/L).

Sterile samples were incubated 18 hours of test tubes containing 10 mL culture of *Escherichia coli*. Culture was obtained from a volume of 10 mL sterile culture medium. The sterile medium was inoculated with 100 µL of *Escherichia coli* (1 %). Once obtained 10 mL of culture were placed over the samples. Optical density was determined after 18 hours of incubation. Incubation was performed in the incubator Laboshake Gerhardt.

The bacterial growth was determined by measuring optical density for the four samples and control (*Escherichia coli* without Ti sample) at 600 nm using UV-VIS spectrophotometer (Jenway Spectrophotometer).

2.3.4 Cytotoxicity of TiO_2 ceramic coatings

L929 mouse fibroblast cells (kindly provided by Dr. Ronald Doyle, University of Louisville School of Medicine, Louisville, KY, USA) were cultured overnight (37^oC, humidified atmosphere with 5% CO_2) in flat-bottom 96-well tissue culture plates at a concentration of 10^5 cells/mL in Dulbecco's Modified Eagle's Medium (DMEM) (Sigma-Aldrich, Inc. St. Louis, MO) supplemented with 10% fetal bovine serum (FBS) (BIOCHROM AG, Berlin, Germany) and 100 U/mL penicillin-streptomycin (Lonza, Verviers, Belgium). When cells reached 85–90% confluence they were detached by trypsin (Sigma–Aldrich), collected and used for cytotoxicity assay. *In vitro* cytotoxicity assay was described in previous study [36]. Control samples optical density was considered as 100% viability. Experiments were performed in triplicate.

3. Results and discussion

3.1. Surface characterization

3.1.1. Scanning electron microscopy analysis

Fig. 1 (a-c) shows SEM micrographs of the surfaces of titanium substrates modified by PEO at 250V, 350V, 450V for 3 minutes, in the Ca and P containing solution. Due to a high temperature in discharge channels during the PEO process a porous and rough surface with micropores is formed.

The TiO_2 coatings obtained at 250 V exhibited a porous microstructure with small pores which are well distributed homogeneously over the samples. It can be observed that the pore became larger with increasing applied voltage, due to the electrical sparks, which are responsible for pores formation. These are weaker at low voltages due to low current passing through the electrochemical cell. In contrast, the electrical sparks become stronger at higher applied voltages, determining the apparition of larger pores on the surface. These results are consistent with those obtained by other researchers [37-39].

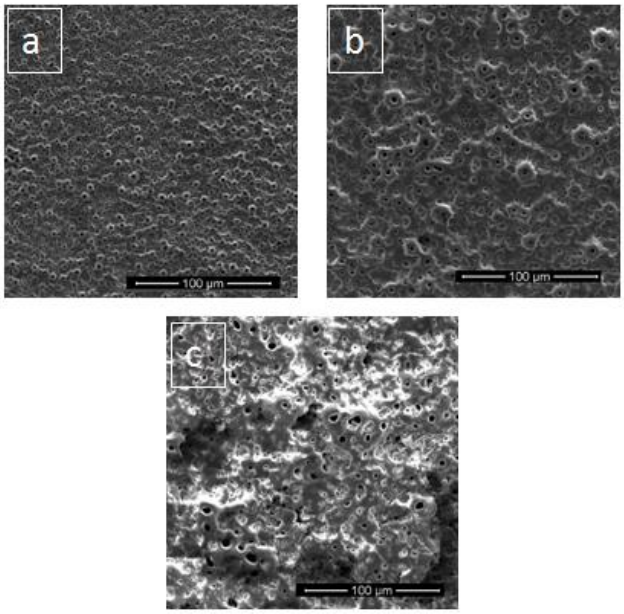

Fig. 1 SEM surface morphologies of titanium samples modified by PEO at: a) 250V; b) 350V; c) 450V

Consequently, the highest voltage values used for PEO treatment leads to the formation of oxide films on Ti, the surfaces becoming irregular and rough with voltage increasing (Fig. 1c).

3.1.2 AFM analysis

The 2D and 3D AFM images of the treated and untreated titanium surfaces are presented in the Fig. 2. The samples modified by PEO show an important increase of

roughnes up to 303 nm for sample treated at 250V, 502 nm for sample treated at 350V and 565 nm for sample treated at 450V compared with untreated Ti surface which presents a roughness of only 59 nm (Table 1).

Table 1. The roughness of titanium surfaces treated and untreated with PEO

Sample	Rms (nm)
Ti untreated	59,8
250 V	303
350 V	502
450 V	565

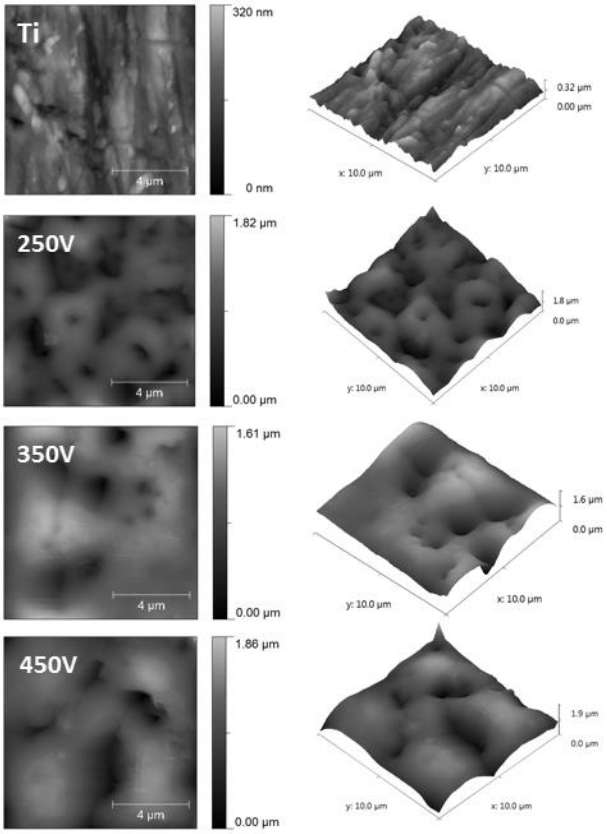

Fig. 2 2D and 3D AFM images of the untreated Ti surface and PEO modified Ti at 250V, 350 V, 450 V

The surface topography is also changed after PEO treatment showing a microporous structure with different pore dimension depending on applied voltage.

The pore shape also differs depending on the treatment, varying from a porous structure in the form of circular nest with diameters less than 1 µm, for the sample obtained at 250 V to a porous structure in the form of larger cavities for higher voltage treatments. The treatment performed at 450 V leads to the changing of the pore shape from the circular to elongate with one dimension of 2 – 4 µm.

3.1.3 EDX measurements

The bioactivity of coverage depends on some physicochemical parameters such as hardness, porosity, phase and elemental composition and bond strength [5].

The elemental composition for titanium substrate PEO modified was identified with the EDX characterization technique (Fig. 3).

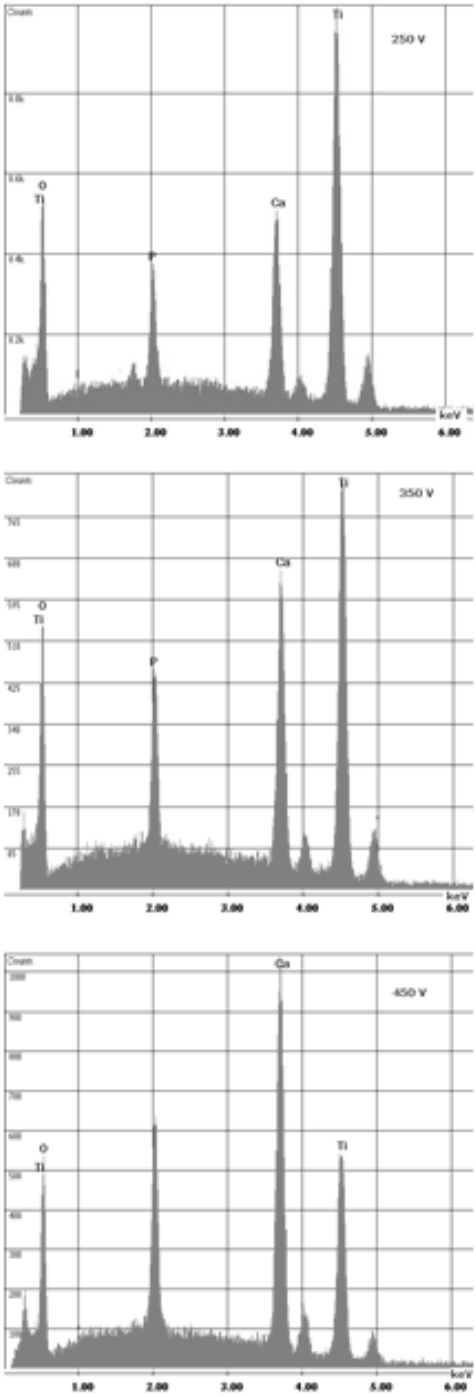

Fig. 3 EDX spectra of TiO_2 films prepared at 250V, 350V and 450V

In the composition of films were identified titanium, oxygen, calcium and phosphorus. From Table 2, showing the EDX analysis performed on the coatings described above, can be observed that while the voltage increased, the oxygen and titanium content is reduced, favoring the increasing of calcium and phosphorus percentage.

Table 2. Relative content of O, Ca, P for the PEO treated titanium

Sample	Relative content			
	O (at.%)	Ca (at.%)	P(at.%)	Ca/P
250 V	57,46	8,81	4,79	1,83
350 V	56,94	12,90	5,87	2,19
450 V	50,15	18,88	7,65	2,46

The Ti coatings that have an appropriate Ca and P content are recommended to be used as biomimetic implant materials in bone tissue applications because Ca and P element introduced during PEO could increase the opportunity to form hydroxyapatite. In particular, the phase composition and the ratio Ca / P of the formed layer should be near the hydroxyapatite (Ca / P = 1.67), which is a main component of bone tissue. The study of Yang et al. [40] revealed that the bioactivity of the coatings was improved as the Ca/P ratio overcome those of existing in HA. Furthermore, Mohedano et al. [41] stated that the presence of Ca and P in TiO_2 coating with a Ca/P ratio exceeding that of any stoichiometric Ca–P–O and Ca–P–O–H compounds, facilitates faster osteoblast cell adhesion. This finding has important significance for developing the bioactivity of Ti implant materials.

3.1.4 XRD measurements

Ca and P elements determined using EDX analyze enter in the composition of different compounds formed during the PEO process. In the study of Abbasi et al. [42], after a PEO process applied for Ti substrate, $CaTiO_3$ and $Ca_3(PO_4)_2$ are supposed to be by-products of the chemical reactions which occurred in high temperature resulted due to electrical discharges on the surface, during formation of TiO_2 coating. These two products could be generated through the reaction between HAp and TiO_2.

In Fig. 4 are presented the XRD diagrams (θ / 2θ) of coatings 250 V, 350 V and 450 V of the titanium treated substrates. The intensity is represented in arbitrary units.

For the TiO_2 obtained at 250 V, only peaks of anatase phase could be observed. The content in rutile phase is insignificant. For the coating obtained at 350 V is observed an increase in rutile phase. The anatase and rutile peaks have almost the same intensity.

As EDX analyze confirmed, Ca and P are present in all samples but the degree of crystallinity of calcium containing compounds increase with applied voltage. The peaks corresponding to HAp, α - $Ca_3(PO_4)_2$ and $CaTiO_3$ are hardly visible at 250 V, begin to rise at 350V and are more evident at 450 V when the crystalizing process is more intense.

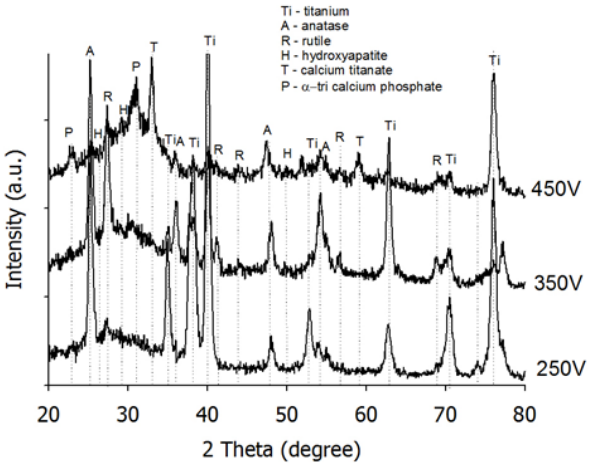

Fig. 4 XRD patterns of the PEO coatings deposited at different voltages.

Therefore, the composition of the coatings obtained by PEO at 450 V contains a mixture of crystalline phases: rutile, anatase, $CaTiO_3$, the α - of $Ca_3(PO_4)_2$ and HAp.

The $CaTiO_3$ phase appears due to the increase in reaction energy. One interesting characteristic from X-ray diffraction analyze results is the formation of tricalcium phosphate at higher voltage (450 V), which is a well-known bioresorbable phase of calcium phosphate [43].

In another study, after the heat-treatment of the PEO coating, a $CaTiO_3/TiO_2$ composite (CTC) coating was also reported [44]. In recent years, $CaTiO_3$ compound has attracted much attention in the field of biomedical materials. The formation of $CaTiO_3$ was also reported during the preparation of HAp coating on titanium and it has been proposed as an intermediate layer to improve the adhesion between HAp and substrate, thus generating an important potential application in the biomedical field. [44-46].

3.1.5 FTIR analysis

The FT-IR spectra of the PEO coating are shown in Fig. 5. The vibration band of phosphate (P–O) was observed for all PEO coatings. This band became more intense at higher voltage, when more Ca and P coatings are entrapped.

In the FT-IR spectrum, absorption peaks of PO_4 bands were observed including the triply degenerated asymmetric stretching mode of PO_4 band at 1033 cm^{-1}. Moreover, the weak OH^- stretch band in the spectrum at around 3550 cm^{-1} may be due to the presence of apatite in the coatings.

The FTIR analyse confirm the observation from XRD studies, revealing the presence of PO_4 containing compounds.

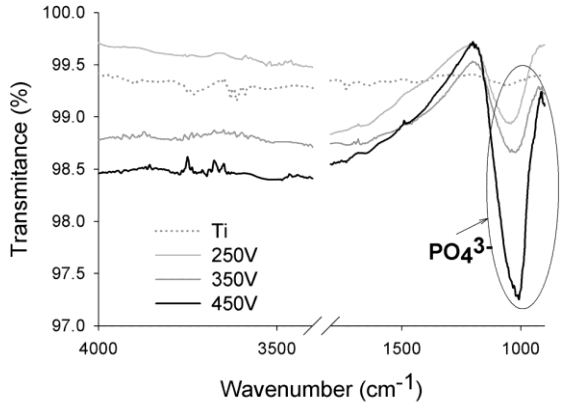

Fig. 5 FTIR spectra for Ti and the Ti samples modified by PEO at 250V, 350V, 450V

3.1.6 Surface wettability

On a textured surface, the equilibrium state of a water droplet is strongly dependent on the surface chemistry and on the topography. However, when the surface chemistry favors partial wetting, topography can result in a droplet spreading completely. Considering this aspect, the water contact angles measured for PEO deposited coatings was discussed in terms of the Cassie–Baxter and Wenzel models [47]. Normally, a liquid droplet deposited on a solid surface establishes a defined equilibrium contact angle. Particularly, in the case of textured surfaces, the ideal Young's relation is not fulfilled. If the droplet remains on top of the textured surface, with trapped air underneath, it is Cassie–Baxter model. In this model, for hydrophobic substrate (contact angle > 90°), contact angle increases with the average roughness. If the liquid is in contact with the entire exposed surface, it is the Wenzel state. In this state, hydrophilic substrate (contact angle < 90°), becomes more hydrophilic with a higher average roughness. The samples discussed in this study fits in this Wenzel state, since the contact angle values for TiO_2 coatings varied around the hydrophobic/moderate hydrophylic limit, from 98° to 71° showing an increase in hydrophilicity of surfaces after the PEO treatment: the water contact angle decreased once the applied voltages increased, as can be observed in Table 3. This effect is based mostly on the modifications produced in surface topography, the Ti surface becoming rougher as TiO_2 was grown on the surface at higher voltage. The anatase/rutile content may affect, also, the hydrophobicity of the coatings. Moreover, a decrease in the contact angle values, from 98.44 to 70.99 is associated with a more hydroxyl rich surface, resulted after the formation of hydroxyapatite.

Table 3. The values water contact angle for the PEO treated samples

Sample	250V	350V	450V
Contact angle (°)	98.44	92.43	70.99

3.1.7 Adherence test

The adhesion of a bioactive film on a substrate is an important aspect to be considering, since it is subjected to mechanical stress, specially - friction. If analysed separately: hydroxyapatite, despite its good bioactivity, is not suitable for load-bearing conditions because of its poor mechanical properties. As compared to these fragile ceramics, metal materials exhibit excellent mechanical toughness and strength. However, they exhibit poor bioactivity. Thus, the ideal solution comes from combining this two materials: deposition/inclusion of bioactive coatings on titanium as an approach to solve the disadvantages of ceramic and metal biomaterials. Moreover, in the case of this study, the ceramic material was included in the TiO_2 coating deposited on Ti substrate, thus, obtaining an adherent coating. The adherence strength of the coating containing TiO_2, Ca and P was appreciated using an adherence test.

Three TiO_2 films were deposited on Ti substrate, in the conditions mentioned in the experimental section. The results presented in Fig. 6 reveal that the most adherent coating is that obtained at 350V. These results are very promising since improving the adherence of hydroxyapatite on a substrate represented until now a difficult issue to solve [48].

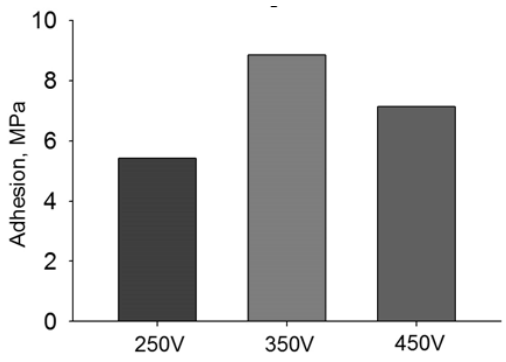

Fig. 6 Adherence test for TiO_2 films deposited onTi substrate using PEO technique.

3.2. Electrochemical characterization

In the case of a medical device, the corrosion resistance is one of crucial factors that influences the future success of the implant, assuring its role for a long period of time.

Cyclic voltammetry

The electrochemical behavior was tested in buffer solution for the Ti/TiO_2 samples obtained at 250, 350 and 450V. The cyclic voltammetry curves for all four samples are comparatively presented in Fig. 7. The current density low values of for all Ti/TiO_2 samples compared with those of Ti substrate, denote the protective roll of TiO_2 films. The appearing peak at 2V for Ti and 250V samples indicates the presence of a transition state from Ti^{3+} to Ti^{4+}. Then, the current plateau of about 150 μA/cm^2 for Ti

and 20 μA/cm^2 for 250V, highlights the continuing consolidation of the oxide layer.

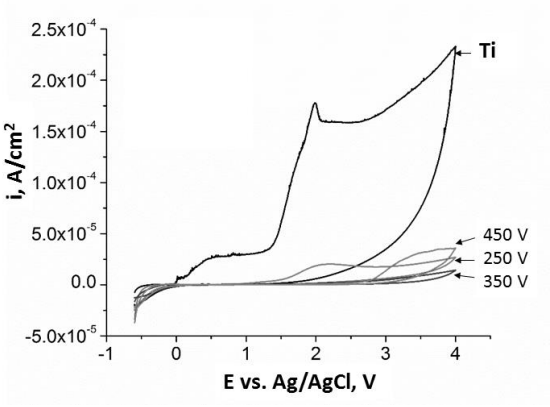

Fig. 7 Cyclic voltametry curves for Ti substrate and Ti/TiO_2 films obtained at 250V, 350V and 450V

For other samples, obtained at 350V and 450V, this transition is not observed, and any other oxidative processes are not visible in the potential range 0 – 3 V, suggesting a better stability of TiO_2 films obtained at higher voltage. For sample 350V the current remains almost constant even up to 4 V.

Tafel plots

The results from Tafel plots, obtained at initial immersion time in buffer solution, for Ti substrate sample, and 250V, 350V and 450V samples are presented in Fig. 8 and Table 4.

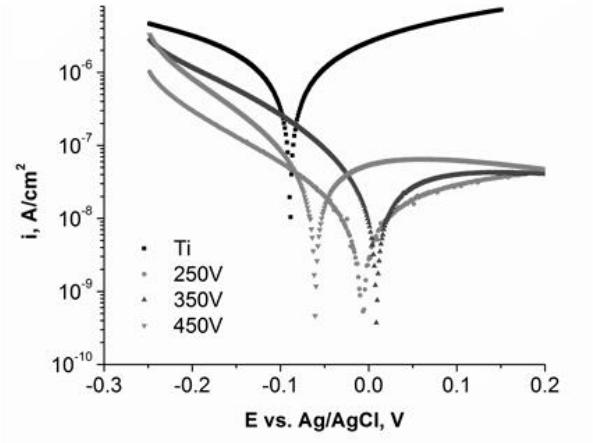

Fig. 8 Tafel plots for Ti and Ti/TiO_2 samples obtained at 250V, 350V and 450V.

The growth of TiO_2 films on the titanium substrate obtained by PEO leads to an important improving of the corrosion parameters. The corrosion potential for the samples covered with TiO_2 was slightly displaced to more electropositive values and the current densities values were reduced from 8 μA/cm^2 to current densities that are in nanometric range.

Table 4. Electrochemical parameters for the Ti and Ti/TiO_2 films from Tafel plots

Sample	E_{corr}, (V)	J_{corr} (nA/cm^2)	Polarization resistance (MΩ)	Corrosion rate (mm/year)
Ti	-0.0865	8208	0.0348	$714 \cdot 10^{-4}$
250V	-0.0721	56.16	2.5949	$4.88 \cdot 10^{-4}$
350V	+0.0089	54.94	1.0996	$4.78 \cdot 10^{-4}$
450V	-0.0593	187.96	0.6768	$16.3 \cdot 10^{-4}$

Another important parameter is the corrosion rate that decreases considerably from $7.14 \cdot 10^{-2}$ mm/year for Ti substrate to values that are two order of magnitude lower, between 4.88 and $16.3 \cdot 10^{-4}$ mm/year for Ti/TiO_2 samples. Thus, these TiO_2 films improve the corrosion parameters by better isolating the metal from the corrosive environment, suppressing the anodic dissolution of the metal.

Nevertheless, if the corrosion parameters of the three Ti/TiO_2 samples are compared, the most corrosion resistant are the samples obtained at 250 and 350V. The third sample, obtained at 450V is probably less resistant than the other two TiO_2 samples because of the bigger dimensions of the pores in the TiO_2 film, that leads also to a decrease in polarization resistance.

All the samples have a lower corrosion rate compared with untreated Ti substrate, strengthening the observations drawn from cyclic voltammetry.

Electrochemical impedance spectroscopy

The impedance spectra of the untreated Ti and Ti/TiO_2 samples modified surface by PEO are used to determine some electrochemical parameters at the interface Ti/TiO_2 - electrolyte.

The Nyquist diagrams for untreated Ti and Ti/TiO_2 samples are presented in Fig. 9. The equivalent circuits proposed according to the impedance spectra are also presented in Fig. 9, for each sample.

The electrolyte solution resistance was noted as Rs in all proposed circuit. For the Ti surface the observed incomplete charge-transfer semicircle corresponds to RQ parallel combination, and is associated with the resistance of native oxide TiO_2 thin film (R1), in parallel to the first constant phase element (Q1). For all Ti/TiO_2 surfaces, other RQ parallel combination (R2 in parallel to the second constant phase element, Q2), was added in circuit corresponding to TiO_2 film formed after the PEO treatment

Electrical parameters of the proposed equivalents circuits obtained after results fitting are presented in the Table 5.

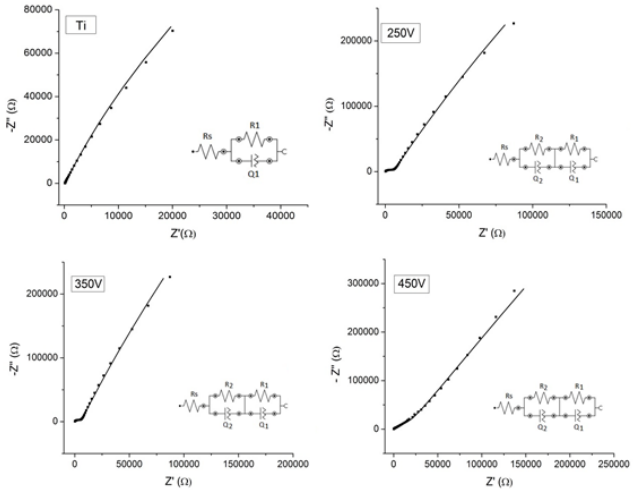

Fig. 9 Nyquist spectra for uncoated Ti and modified Ti with PEO at 250V, 350V and 450V

The resistance R1 which was associated, for Ti sample, with the native oxide film formed instantly on its surface, is about 1.06 MΩ. For Ti/TiO_2 sample obtained by PEO treatment, R1 is associated with the inner oxide layer from the titanium – oxide interface which is expected to be more compact (less porous). The values of R1 increase, after PEO treatment, reaching at 5.6 MΩ for 250V, 60 MΩ for 350V and 25.9 MΩ for 450V, respectively.

The resistance R2 which is associated, for Ti/TiO_2 sample, with the outer oxide layer, is three orders of magnitude lower comparing with R1. This difference is due to outer porous oxide layer as was highlighted from SEM and AFM analysis. The order of R2 resistances is similar with that observed for R1, $R_{250V} < R_{450V} < R_{350V}$.

Table 5. Electrical parameters of the proposed equivalents circuits.

Parameters	Rs	R1	CPE1	R2	CPE2		
Units	Ω	kΩ	μMho	n	MΩ	μMho	n
Ti	135	-	-	-	1.060	19.8	0.876
Ti-250V	128	5.45	0.401	0.829	5.64	6.10	0.819
Ti-350V	148	60.3	0.203	0.881	60	5.81	0.765
Ti-450V	120	15.6	2.68	0.655	25.9	4.41	0.734

Thus, the higher resistance values were obtained for 350V, beeing in a good correlation with the Tafel results, which revealed the lowest corrosion rate, and CV curves, which also revealed lowest anodic current for this sample.

For 450V sample, obtained at highest voltage, the TiO_2 film resistance is lower comparing 350V showing that the increasing in pore dimension can facilitate the liquid penetration affecting the corrosion resistance.

The values of CPE2 coefficient, n, sustain this observation, beeing closer toward the diffusive behavior for 450V (0.65) and pseudocapacitive behaviour for 350V (0.88).

3.3. Antibacterial activity

The bacteriological experiments performed *in vitro* demonstrated the effectiveness of TiO_2, Ca and P containing coatings in inhibiting the growth of *Escherichia coli* bacteria (Table. 6). The antibacterial activities of coatings were determined by calculating the percentage inhibition of growth using the formula [49]:

$$I\ \% = [(B_{18} - B_0) - (C_{18} - C_0)]/ (B_{18} - B_0) \cdot 100 \qquad (1)$$

where I is the percentage inhibition of growth , B_{18} is the blank- compensated optical density at 600 nm OD_{600} = 3.36 of the positive control of the organism at 18 h, B_0 is the blank-compensated OD_{600} of the positive control of the organism at 0 h (OD_{600} = 0.049), C_{18} is the negative control-compensated OD_{600} of the organism in the presence of test sample at18 h and C_0 is the negative control-compensated OD_{600} of the organism in the presence of test sample at 0 h (OD_{600} = 0.049).

Table 6 shows the average optical density in three experiments conducted according to the above description and the percentage inhibition of growth for the four samples.

Table 6. Percentage inhibition of bacteria growth, %

Sample	**C_{18}**	**I, %**
250V	0.93	83
350V	0.96	82
450V	0.95	82
Ti control	2.68	20

The results indicated that the samples prepared in this study possess strong antibacterial activity.

This is attributed to the increase in amount of crystalline titanium dioxide available to participate in the photocatalytic reaction as well as to the increase of high photocatalytic crystalline phase of anatase and rutile.

It was demonstrated that the killing mechanism of TiO_2 to microorganism is caused by the oxidizing reaction of the reactive oxygen species. Therefore, it is reasonable that TiO_2 producing a larger amount of hydroxyl radicals showed greater antibacterial activity.

However, among these reactive oxygen species, which species are directly involved in the damage of bacterial cells or which species contribute more to the oxidative reactions with organic compounds is still subject to investigation. The endotoxin is a component of the outer membrane of gram negative bacteria and is released only when the cellular structure is destroyed. The results indicated that the TiO_2 destroys the outer membrane of the *E. coli* cell and causes the death of the bacteria.

The researchers believe the cell death was caused by the decomposition of the cell wall first, and then subsequent decomposition of cell membrane. Damage of the cell membrane directly leads to leakage of minerals, proteins, and genetic materials, causing cell death [50].

3.4. Cells cultivation

In vitro biocompatibility of samples was assessed by measuring L929 cells viability through the MTT assay. Samples were incubated for 24 h in Phosphate Buffer Saline (PBS) to allow leakage of potential cytotoxic compounds and, subsequently, supernatants were brought into contact with the adhered cells overnight. MTT assay was performed on test samples, each determination representing three replicates. Cells response to PBS was considered as positive control (100% cell viability).

Results show no noticeable difference between samples and, moreover, there is no sign of cytotoxicity of either sample in terms of leaked components, as observed in Fig. 10. Further studies are needed to certify the *in vivo* biocompatibility of these formulations.

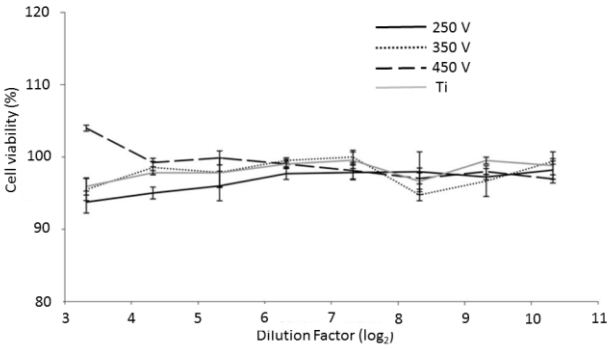

Fig. 10 Cytotoxic effect of untreated Ti and Ti samples modified with PEO

Correlating the results from cytotoxic test with those from surface characterisation, it can be concluded that the new coatings based on PEO sinthesized TiO_2 have a good electrochemical behaviour in terms of corrosion resistance and the appropriate topography and wettability to be used as a coating for titanium, in biomedical applications.

4. Conclusions

The titania coatings containing Ca and P was successfully prepared on titanium substrat using plasma electrolytic oxidation technique. The highest voltage values used for PEO treatment leads to the formation of a porous oxide films on Ti. The surface topography presents a microporous structure with different roughness and pore dimension, depending on applied voltage.

An increase in calcium and phosphorus percentage was favored by high voltage values. The composition of the coatings obtained by PEO at 450 V contains a mixture of crystalline phases: rutile, anatase, $CaTiO_3$, the alpha phase of $Ca_3(PO_4)_2$ and HAp. The characteristics of the FTIR spectra confirmed the presence of PO_4^{3-} containing compounds on the TiO_2 coatings. The contact angle values for TiO_2 coatings varied around the hydrophobic to moderate hydrophylic limit, from 98° to 71°. The most adherent coating on Ti substrate was obtained at 350V.

The low values of current density for all Ti/TiO_2 samples compared with those of Ti substrate, denote the protective roll of TiO_2 films. The growth of TiO_2 films on the Ti substrate obtained through the PEO leads to an important improving of the corrosion parameters. The most corrosion resistant are the samples obtained at 350V.

The results indicated that the samples prepared in this study possess strong antibacterial activity and there is no sign of cytotoxicity of either sample in terms of leaked components, conferring them an important potential application in the biomedical field.

Acknowledgements

The authors are grateful to Moga Sorin, for assistance with XRD measurements.

References

[1] A. Zielinski, S. Sobieszczyk, Corros. Rev. **26**, 1 (2008).
[2] T. Hryniewicz, R. Rokicki, K. Rokosz, Surf. Coat. Tech. **203**, 1508 (2009).
[3] R. Bhola, S. M. Bhola, B. Mishra, D. L. Olson, Trends Biomater. Artif. Organs **25(1),** 34 (2011).
[4] A. Mahapatro, J. of Biomater. Tiss. Eng. **2**, 259 (2012).
[5] X. Y. Liu, P. K. Chu, C. X. Ding, Mat. Sci. Eng R **47**, 49 (2004).
[6] A. Mahapatro, Mater. Sci. Eng. C **55**, 227 (2015).
[7] X. Y. Liu, P. K. Chu, C. X. Ding, Mat. Sci. Eng R **70**, 275 (2010).
[8] M. Lorenzetti, E. Pellicer, J. Sort, M. D. Baro, J. Kovac, S. Novak, S. Kobe, Materials, **7**, 180 (2014).
[9] J. Pan, C. Leygraf, D. Thierry, A. M. Ektessabi, J. Biomed. Mater. Res. **35**, 309 (1997).
[10] S. Popescu, I. Demetrescu, C. Sarantopoulos, A. N. Gleizes, D. Iordachescu, J. Mater. Sci.-Mater. M. **18,** 2075 (2007).
[11] A. W. Tan, R. Ismail, K. H. Chua, R. Ahmad, S. A. Akbar, B. Pingguan-Murphy, Appl. Surf. Sci. **320**, 161 (2014).

[12] H. Lee, S. Dregia, S. Akbar, M. Alhoshan, J. Nanomater. **ID 503186**, 7 (2010).
[13] C. Dumitriu, C. Pirvu, I. Demetrescu, J. Electrochem. Soc. **160**, G55 (2013).
[14] G. A. Crawford, N. Chawla, K. Das, S. Bose, A. Bandyopadhyay, Acta Biomater. **3**, 359 (2007).
[15] M. Tallarida, D. Friedrich, M. Stadter, M. Michling, D. Schmeisser, J. Nanosci. Nanotechno. **11**, 8049 (2011).
[16] P. Schindler, M. Logar, J. Provine, F. B. Prinz, Langmuir **31**, 5057 (2015).
[17] M. R. Bayati, F. Golestani-Fard, A. Z. Moshfegh, Mater.Chem. Phys. **120**, 582 (2010).
[18] H. Cimenoglu, M. Gunyuz, G. T. Kose, M. Baydogan, F. Ugurlu, C. Sener, Mater. Charact. **62**, 304 (2011).
[19] P. Huang, F. Wang, K. W. Xu, Y. Han, Surf. Coat. Tech. **201**, 5168 (2007).
[20] E. Matykina, A. Berkani, P. Skeldon, G. E. Thompson, Electrochim. Acta **53**, 1987 (2007).
[21] Y. W. Lim, S. Y. Kwon, D. H. Sun, H. E. Kim, Y. S. Kim, Clin. Orthop. Relat. R **467**, 2251 (2009).
[22] L. H. Li, Y. M. Kong, H. W. Kim, Y. W. Kim, H. E. Kim, S. J. Heo, J. Y. Koak, Biomaterials **25**, 2867 (2004).
[23] E. Vanderleyden, S. Van Bael, Y. C. Chai, J. P. Kruth, J. Schrooten, P. Dubruel, Mat. Sci. Eng. C-Materials for Biological Applications **42**, 396 (2014).
[24] C. Chen, S. M. Zhang, I. S. Lee, Surf. Coat. Tech, **228**, S312 (2013).
[25] R. Tejero, E. Anitua, G. Orive, Prog. Polym. Sci. **39**, 1406 (2014).
[26] Q. L. Huang, X. Yang, R. R. Zhang, X. J. Liu, Z. J. Shen, Q. L. Feng, Ceram. Int. **41**, 4452 (2015).
[27] A. Krzakala, A. Kazek-Kesik, W. Simka, Rsc Advances **3**, 19725 (2013).
[28] D. Dzhurinskiy, Y. Gao, W. K. Yeung, E. Strumban, V. Leshchinsky, P. J. Chu, A. Matthews, A. Yerokhin, R. G. Maev, Surf. Coat. Tech. **269**, 258 (2015).
[29] J. Z. Chen, Y. L. Shi, L. Wang, F. Y. Yan, F. Q. Zhang, Mater. Lett. **60**, 2538 (2006).
[30] J. H. Ni, Y. L. Shi, F. Y. Yan, J. Z. Chen, L. Wang, Mater. Res. Bull. **43**, 45 (2008).
[31] S. Abbasi, F. Golestani-Fard, H. R. Rezaie, S. M. M. Mirhosseini, A. Ziaee, Mater. Res. Bull. **47**, 3407 (2012).
[32] M. Hekmatfar, S. Moshayedi, S. A. Ghaffari, H. R. Rezaei, F. Golestani-Fard, Mater. Lett. **65**, 3421 (2011).
[33] X. L. Zeng, J. F. Li, S. H. Yang, Q. X. Zheng, Z. W. Zou, Appl. Surf. Sci. **258**, 4489 (2012).
[34] C. Massaro, M. A. Baker, F. Cosentino, P. A. Ramires, S. Klose, E. Milella, J. Biomed. Mater. Res. **58**, 651 (2001).
[35] R. H. U. Khan, A. L. Yerokhin, X. Li, H. Dong, A. Matthews, Surf. Eng. **30**, 102 (2014).
[36] S. Popescu, C. Ungureanu, G. Purcel, V. Tofan, M. Popescu, A. Sălăgeanu, C. Pîrvu, Mat. Sci. Eng. C **42**, 726 (2014).
[37] Y. K. Shin, W. S. Chae, Y. W. Song, Y. M. Sung, Electrochem. Commun **8**, 465 (2006).
[38] M. R. Bayati, R. Molaei, A. Kajbafvala, S. Zanganeh, H. R. Zargar, K. Janghorban, Electrochim. Acta **55**, 5786 (2010).
[39] S. Abbasi, M. R. Bayati, F. Golestani-Fard, H. R. Rezaei, H. R. Zargar, F. Samanipour, V. Shoaei-Rad, Appl. Surf. Sci. **257**, 5944 (2011).
[40] X. L. Yang Z., li W. and J. Han, J. Adv. Biomed Eng Techn. **2**, 13 (2015).
[41] M. Mohedano, R. Guzman, R. Arrabal, J. L. Lacomba, E. Matykina, J. Biomed. Mater. Res. B **101**, 1524 (2013).
[42] S. Abbasi, F. Golestani-Fard, H. R. Rezaie, S. M. M. Mirhosseini, Appl. Surf. Sci. **261**, 37 (2012).
[43] L. L. Hench, J. Am. Cer. Soc. **74**, 1487 (1991).
[44] D. Q. Wei, Y. Zhou, D. C. Jia, Y. M. Wang, J. Biomed. Mater. Res. B **84B**, 444 (2008).
[45] C. S. Chien, T. Y. Liao, T. F. Hong, T. Y. Kuo, C. H. Chang, M. L. Yeh, T. M. Lee, J. Med. Biol. Eng. **34**, 109 (2014).
[46] R. Shi, C. Bai, M. Hu, X. Liu, J. Du, J. Min. Metall. Sect. B, **47**, 99 (2011).
[47] V. C. Anitha, J. H. Lee, J. Lee, A. N. Banerjee, S. W. Joo, B. K. Min, Nanotechnology **26**, 065102 (2015).
[48] C. J. Chung, R. T. Su, H. J. Chu, H. T. Chen, H. K. Tsou, J. L. He, J. Biomed. Mater. Res. B **101B**, 1023 (2013).
[49] S. Jaiswal, B. Duffy, A. K. Jaiswal, N. Stobie, P. McHale, Int. J. of Antimicrob. Ag. **36**, 280 (2010).
[50] G. F. Fu, P. S. Vary, C. T. Lin, J. Phy. Chem. B **109**, 8889 (2005).

*Corresponding author: s_popescu@chim.upb.ro, popescu.sa@gmail.com